Apparent Activation Energies Associated with Protein Dynamics on Hydrophobic and Hydrophilic Surfaces

Blake B. Langdon, Mark Kastantin, and Daniel K. Schwartz*
Department of Chemical and Biological Engineering, University of Colorado Boulder, Boulder, Colorado

ABSTRACT With the use of single-molecule total internal reflection fluorescence microscopy (TIRFM), the dynamics of bovine serum albumin (BSA) and human fibrinogen (Fg) at low concentrations were observed at the solid-aqueous interface as a function of temperature on hydrophobic trimethylsilane (TMS) and hydrophilic fused silica (FS) surfaces. Multiple dynamic modes and populations were observed and characterized by their surface residence times and squared-displacement distributions (surface diffusion). Characteristic desorption and diffusion rates for each population/mode were generally found to increase with temperature, and apparent activation energies were determined from Arrhenius analyses. The apparent activation energies of desorption and diffusion were typically higher on FS than on TMS surfaces, suggesting that protein desorption and mobility were hindered on hydrophilic surfaces due to favorable protein-surface and solvent-surface interactions. The diffusion of BSA on TMS appeared to be activationless for several populations, whereas diffusion on FS always exhibited an apparent activation energy. All activation energies were small in absolute terms (generally only a few k_BT), suggesting that most adsorbed protein molecules are weakly bound and move and desorb readily under ambient conditions.

INTRODUCTION

Protein adsorption at the solid-liquid interface is fundamental to many applications, including biocompatible materials, biofilm fouling, biosensing, and protein separations (1,2). The breadth of applications for this very common yet complex phenomenon has spurred diverse and abundant research (3,4), yet a complete mechanistic understanding of dynamic surface behaviors is lacking. Fundamentally, interfacial protein dynamics can involve adsorption, surface diffusion, conformational changes, protein-protein aggregation, and desorption. These dynamics are influenced by four types of binary interactions: protein-solvent, surface-solvent (relative to solvent-solvent), protein-surface, and protein-protein (2,5).

Hydrophobic effects are commonly believed to play a prominent role in protein-surface interactions by influencing the reversibility of binding. For example, both the extent of protein adsorption and the degree of protein unfolding are thought to correlate directly with the surface hydrophobicity (4,6,7). However, recent studies have resulted in a more nuanced view of this assertion by demonstrating the effects of protein concentration on protein unfolding (e.g., lower surface coverage allows easier surface reorientation and greater unfolding) (8–11). Other studies have specifically focused on the behavior of strongly bound protein populations (i.e., protein that is not removed by rinsing) (12,13). For example, Fainerman et al. (12) calculated the activation energy for protein desorption from the air-water interface and concluded that protein adsorption is thermodynamically reversible but may appear kinetically irreversible due to slow desorption rates.

Conventional methods that are widely used to study interfacial protein behavior include solution depletion (14), surface plasmon resonance (15,16), quartz crystal microbalance (2), ellipsometry/reflectometry (17,18), and fluorescence recovery after photobleaching (13). These techniques are limited in their ability to provide direct mechanistic insights (19). For example, these methods measure only the net effects (e.g., total coverage) associated with multistep mechanisms, so interpretations based on these methods are highly model-dependent (20). Also, they measure only the ensemble average behavior under conditions that are recognized to be heterogeneous, e.g., proteins exist in a range of states associated with conformation, orientation, and/or aggregation. These experimental limitations (and the desire to infer molecular mechanisms from these data) have unfortunately led to a field that is fraught with examples of overinterpretation, and a "conventional wisdom" that is often unsupported by empirical data. It is often said that certain types of surfaces (e.g., hydrophobic surfaces) "cause" protein unfolding and irreversible adsorption, whereas other surfaces (e.g., polyethylene glycol brushes) are "protein-resistant". However, several alternate hypotheses are consistent with the net ensemble-average behavior that has been measured on such surfaces. For example, it is equally possible that hydrophobic surfaces act as "collectors" of rare unfolded/aggregated populations that exist in solution. Similarly, there is little evidence that polyethylene glycol surfaces actually resist adsorption of individual proteins; alternatively, they may influence protein-protein associations in a way that inhibits interfacial aggregation.

In previous work in our laboratory and in other laboratories employing total internal reflection fluorescence microscopy (TIRFM), single-molecule dynamics were imaged at

Submitted February 20, 2012, and accepted for publication April 19, 2012.

*Correspondence: daniel.schwartz@colorado.edu

Editor: Elizabeth Rhoades.

0006-3495/12/06/2625/9 $2.00

doi: 10.1016/j.bpj.2012.04.027

the solid-liquid interface (20–28). Using a single-molecule approach, one can directly observe an individual protein adsorbing, diffusing, and desorbing from the interface. Single-molecule methods are uniquely able to identify and characterize heterogeneous behavior and populations (21–23). For example, Kwok and co-workers (21) identified two populations of bovine serum albumin (BSA) adsorbing to quartz surfaces based on surface residence times. The largest population (99.3% of objects) resided on the surface for <1 min, whereas the second population exhibited much longer residence times. In this work, we separate protein-surface dynamics into distinct populations and elementary modes. Each population or mode is analyzed separately to better elucidate important surface-protein interactions and behaviors that may lead to protein unfolding, aggregation, and surface fouling surfaces.

To address protein-surface interactions on a mechanistic level, previous investigators used ensemble-averaged methods to measure the free energies associated with protein adsorption/desorption on hydrophobic and hydrophilic surfaces (12,14,29,30). Fig. 1 illustrates the conventional view of energies associated with adsorbate-surface interactions. Although it is dramatically oversimplified, this view provides a useful context to frame a discussion of the phenomena presented below. In particular, this diagram suggests that the activation energy associated with desorption can be greater than the free energy of adsorption (ΔE), and that both adsorption and desorption are activated processes. Fig. 1 also illustrates the difference between the activation energy for desorption and the activation energy for surface diffusion, where the latter is associated with the corrugation of the surface interaction potential.

We show here that the true situation is even more complex. Multiple populations and modes are omnipresent in studies of proteins at interfaces, and these populations/modes must be isolated if quantitative measurements of energies are to be mechanistically meaningful. Here, we employed single-molecule TIRFM to measure apparent activation energies associated with specific dynamic mechanisms. We studied two common proteins, BSA and fibrinogen (Fg), on both hydrophilic FS and hydrophobic, trimethylsilane (TMS)-coated FS. These experiments were done at very low adsorbed protein coverage, a condition that is very similar to the initial protein adsorption observed before surface fouling occurs. Under these conditions, protein-protein interactions on the surface are insignificant, allowing us to probe direct effects of surface chemistry on protein binding and mobility.

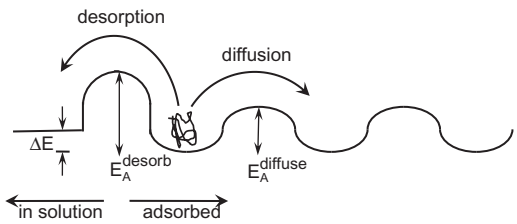

FIGURE 1 Schematic energy diagram illustrating the (simplified) conventional picture of surface adsorption, desorption, and diffusion.

MATERIALS AND METHODS

Protein sample and surface preparation

Fg labeled with AlexaFluor 488 and BSA labeled with AlexaFluor 555 were purchased from Molecular Probes (Eugene, OR). Fg was labeled on average with 15 fluorophores per protein molecule, and BSA was labeled on average with five fluorophores per molecule, as specified by the manufacturer. Phosphate-buffered saline (PBS) at pH 7.2 was purchased from Gibco (Carlsbad, CA). Low surface densities (required for single-molecule experiments) were achieved with the use of protein solutions at concentrations of 10^{-14} and 10^{-12} M on TMS and FS surfaces, respectively. FS wafers were purchased from Mark Optics (Santa Ana, CA). The cleaning and surface functionalization procedures were previously described and are available in the Supporting Material. We verified the surface hydrophobicity of TMS by measuring the static contact angle (e.g., TMS contact angle of 95° ± 3°).

Data acquisition

Protein samples were injected into a temperature-controlled flow cell. Observations at the solid-liquid interface were made under static conditions using TIRFM. Several movies were acquired of each sample, with acquisition times of 200 ms for individual frames. An object-recognition algorithm involving disk matrix convolution followed by thresholding was used to identify diffraction-limited objects as described previously (26). The position of an object was determined by its centroid of intensity. Object tracking between movie frames was accomplished by identifying the closest objects within a 4 pixel (908 nm) distance in sequential frames. Surface residence times were calculated by multiplying the number of frames in which an object was identified by the exposure time of each frame. Further experimental considerations and details are available in the Supporting Material.

Data analysis

We constructed cumulative residence-time distributions by calculating the probability of objects residing on the surface for a time t or greater. Objects with residence times of a single frame were ignored due to the sensitivity of object identification for a single frame to noise. The number of objects with a given residence time were assumed to follow Poisson statistics. The desorption kinetics were assumed to be first-order processes, such that the cumulative residence-time distributions could be described by

$$p(t) = \sum_{i=1} f_i e^{-t/\tau_i}, \quad (1)$$

where $p(t)$ is the probability that a given object has a residence time $\geq t$, and f_i is the relative fraction of all objects represented by population i. Each population had a characteristic surface residence time of τ_i, which is the inverse of that population's effective desorption rate constant ($k_{des,i} = 1/\tau_i$). Orthogonal fitting using the distributed maximum entropy method and discrete maximum likelihood algorithm with the MemExp program (31) confirmed the number of populations used in the above fitting.

We constructed cumulative square-displacement distributions by sorting the displacement data in ascending order and ranking each data point. Interfacial diffusion was assumed to follow 2D random walks with Gaussian statistics. Accounting for positional uncertainty (due to instrument noise) by previously described methods (32), the cumulative squared-displacement distribution can be described by

$$C(R^2, \Delta t) = \sum_{j=1} x_j e^{-R^2/4\left(D_j \Delta t + \sigma^2\right)}, \quad (2)$$

where R^2 is the square-displacement radius given Δt, the time window between observations, x_j is the fraction of observed steps in mode j, D_j is the characteristic diffusion coefficient of mode j, and σ is the positional uncertainty.

We used Eqs. 1 and 2 to fit the experimental cumulative distributions of residence-time and squared-displacement data, respectively, by minimizing the variance weighted by the data point divided by the squared error for the data point.

To determine the apparent activation energy (E_a), we calculated the desorption rate constant (k_{des}) or diffusion coefficient (k_{diff}) for a given population/mode at various temperatures. We then fit these data using the Arrhenius relationship

$$\ln(k) = \frac{-E_a}{R}\frac{1}{T} + \ln(A), \quad (3)$$

where k is the rate constant for diffusion (k_{diff} in units of $\mu m^2\ s^{-1}$) or desorption (k_{des} with units of s^{-1}), R is the universal gas constant, and A is the (variable) preexponential factor whose units reflect those of the rate constant (e.g., a function of μm^2 for diffusion). Further details of the data analysis can be found in the Supporting Material.

RESULTS AND DISCUSSION

Surface dynamics reveals heterogeneous populations and modes

For each protein-surface combination, at least three single-molecule movies (frame time: 200 ms, length: 1500 frames) were obtained at 6°C, 10°C, 15°C, 20°C, 25°C, 30°C, 35°C, and 40°C, respectively. Each object observed in these experiments was characterized by its residence time, mean intensity, and surface trajectory. These data represent >40,000 (BSA on FS), 12,000 (BSA on TMS), 7000 (Fg on FS), and 5000 (Fg on TMS) identified objects, respectively.

Fig. 2 *A* shows typical cumulative surface residence-time distributions for several temperatures. Assuming an exponential decay of residence-time probabilities (as would be observed for first-order desorption kinetics), a homogeneous protein population would appear as a linear relationship with a single characteristic residence time (τ) on the log-linear scaled graph in Fig. 2 *A*. The nonlinearity of the data indicates the presence of multiple populations. This is consistent with previous studies that also found and characterized multiple protein populations (21,22,26,27). At least three exponentials were required to fit each cumulative distribution. We verified the number of distinct populations identified by this method using a convolution of the maximum entropy method and maximum likelihood fitting (described in the Supporting Material) for the same cumulative residence-time fit (Fig. S1) (31). These independent analyses identified the same number of populations for the same cumulative distributions (e.g., four populations for BSA and three for Fg).

As a general rule, the populations identified by surface residence times had certain qualitatively similar characteristics regardless of protein or surface chemistry. Importantly, the fraction of objects observed in the shortest-lived population (characteristic residence time of 0.4–0.7 s) accounted for the majority of objects (~70–80%), and an order of magnitude greater number of objects than was observed in the longest-lived population (characteristic residence time of 9–75 s, 2–9% of objects). The detailed results of fits to cumulative residence-time distributions are shown in Table S1. Using intensity data for each population, we previously demonstrated that each residence-time population roughly corresponded to a different oligomeric state for Fg on TMS or FS and for BSA at the silicone oil-water interface (26,27). Similar connections between residence-time populations and oligomers were explicitly made here for BSA on TMS and FS (Fig. S2).

Due to the statistical distribution of fluorescent labels on a given molecule, some variation is expected in the fluorescence intensity within a given oligomer population. However, this variation is not so large as to preclude identification of monomers, dimers, and trimers. Using the expected Poisson statistics, for example, Fg was labeled with 15 ± 4 fluorophores; dimers and trimers would therefore be expected to have 30 ± 5 and 45 ± 7 fluorophores, respectively, permitting robust resolution of these species. For BSA, which was labeled with 5 ± 2 fluorophores, the separation from dimers (10 ± 3 fluorophores) or trimers

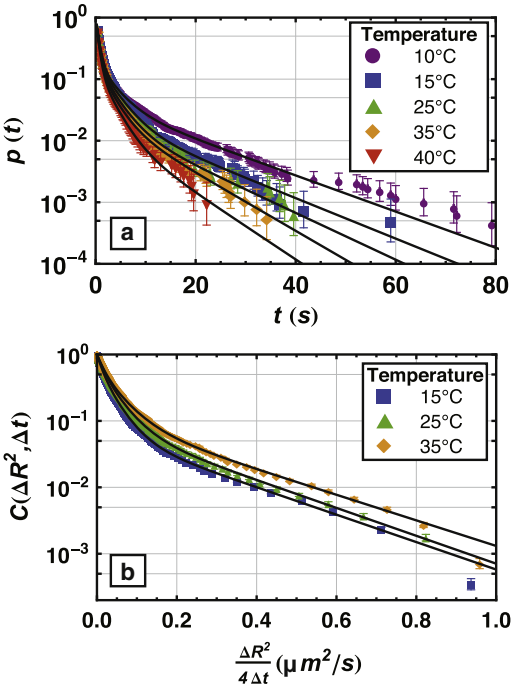

FIGURE 2 Semilog plot of cumulative distributions associated with Fg adsorbed on FS: (*a*) surface residence time probability distributions, and (*b*) squared-displacement distributions. Each data series represents protein dynamics at a different temperature of 10°C, 15°C, 25°C, 35°C, or 40°C. Experimental cumulative distributions are assumed to follow Poisson statistics. The error of each data point represents 68% confidence intervals for a Poisson distribution with mean of that data point.

(15 ± 4 fluorophores) was not as complete, but it was still possible to identify ranges of intensity corresponding to each species.

Analyses of surface residence times provide important insights into the mechanisms that can lead to protein film formation or surface fouling. For example, regardless of protein identity or the nature of the surface, isolated monomeric proteins have extremely short residence times and are unlikely to lead to surface fouling in the absence of productive collisions that can lead to larger oligomers/aggregates with systematically longer surface residence times. This suggests that it is important to understand how collisions/aggregation may occur on surfaces, leading naturally to a discussion of interfacial mobility.

Fig. 2 *B* shows typical cumulative squared-displacement distributions, i.e., the probability of finding the observed molecule beyond a circle of radius R after some time interval, Δt. On this log-linear scaled graph, where cumulative probability is plotted against $R^2/4\Delta t$, diffusion corresponding to a simple 2D random walk would appear as a straight line. These data, which do not appear linear, indicate the presence of multiple interspersed diffusive modes. For most protein-surface combinations, three Gaussian modes were used to fit each movie's cumulative distribution.

Each system exhibited a very fast diffusive mode (M1) with effective diffusion coefficients of 0.23–0.32 $\mu m^2/s$. Generally speaking, the large "flights" associated with this fast mode were uncommon (5–10%), with the exception of Fg on TMS surfaces, where this mode represented nearly 35% of the diffusive steps. The other modes were much slower (effective diffusion coefficients of 0.03–0.05 $\mu m^2/s$ and 0.007–0.014 $\mu m^2/s$ for M2 and M3, respectively). Typically, M2 and M3 both represented substantial fractions of the overall diffusive steps. The detailed results of fits to cumulative squared-displacement distributions are shown in Table S2.

Our direct observation and quantitative analysis of protein mobility at the solid-liquid interface provide direct evidence against the notion that proteins are immobilized upon adsorption. Although the measured diffusion coefficients are much smaller than those observed in solution, they still represent significant mobility. Given the measured diffusion coefficients and residence times, a rough calculation shows that a typical protein object explores an area of ~0.01–0.10 μm^2 between adsorption and desorption, which is thousands of times larger than the molecular footprint of the protein itself. This suggests that even at a very low surface coverage of 10–100 molecules/μm^2, multiple protein molecules will simultaneously be exploring the same region of surface, leading to possible collisions. Thus, one should not think of proteins as being irreversibly immobilized upon adsorption; similarly, random sequential adsorption would appear to be an inappropriate model for protein adsorption. Instead, protein objects remain mobile upon adsorption and can explore significant surface areas before desorption occurs. Some previous reports also emphasized the mobility of adsorbed proteins (13,33–35). These new (to the best of our knowledge) observations should further dispel the misconception of protein immobilization upon adsorption.

In contrast to the residence-time populations, the heterogeneity of the diffusive modes did not correspond directly to protein oligomer populations. In particular, an individual oligomer population often exhibited more than one diffusive mode identified in the total cumulative squared-displacement distribution (Fig. S3). For example, BSA monomers on TMS experienced two diffusive modes with diffusion coefficients 0.048 $\mu m^2/s$ and 0.24 $\mu m^2/s$. The trajectories of brighter objects (i.e., oligomers) were dominated by multiple slow diffusive modes. These observations were similar for both proteins on both types of surface. We speculate that these multiple diffusive modes for a given oligomerization state result from different types of protein associations with the surface, as explored further below.

Rates associated with individual populations/modes increase with temperature

The pervasive heterogeneity described above for both residence-time populations and diffusive modes emphasizes the importance of identifying and analyzing each of these individual elementary mechanisms separately. For example, if one were to analyze the ensemble-averaged desorption rate (or the mean diffusion coefficient) using transition-state theory (12,29), one could extract an effective activation energy; however, this energy would be physically meaningless because it would not correspond to the actual energy of any particular transition state. The temperature dependence of an averaged quantity depends on both changes in the rates of individual modes and changes in the relative fractions of various modes. However, only the temperature dependence of rates associated with individual modes has real physical meaning. For example, previous work showed that diffusion coefficients associated with distinct diffusive modes of surfactants may have different characteristic activation barriers (24).

Fig. 2 *A* shows that the overall residence-time distribution shifted to shorter times as temperature was increased. Similarly, as shown in Fig. 2 *B*, the cumulative squared-displacement distribution shifted to larger displacements with increasing temperature. These changes with temperature could result from two different trends: 1), the fraction of objects associated with each population/mode changes such that the fraction of objects in the shortest-lived population or fastest-diffusing mode increases with temperature; or 2), the characteristic residence times and diffusion coefficients change systematically with temperature. Only the latter effect would indicate that surface dynamics are activated processes. Our observations revealed that the population and mode fractions did not vary over the temperature

range within statistical significance. Instead, the characteristic residence times (i.e., inverse desorption rates) and diffusion coefficients changed systematically with temperature for each population/mode.

Fig. 3 shows Arrhenius plots (i.e., the natural log of the rate constant versus the reciprocal absolute temperature) for the characteristic desorption rate constants of all populations calculated for each protein-surface combination. Again, P1 corresponds to the shortest-lived population (fastest desorption rate), and P2, P3, and P4 correspond to the populations with progressively slower desorption rates. Fig. 4 shows the Arrhenius plots for the diffusion coefficients of diffusive modes associated with each protein-surface combination. These Arrhenius plots show that diffusion also followed Arrhenius behavior (with the exception of M2 for BSA on TMS, which exhibited negligible changes with temperature and will be discussed below in greater detail).

Apparent activation energies of protein-surface dynamics

As described above, an analysis of the temperature-dependence for each dynamic mode, population, and protein-surface combination showed agreement with Arrhenius behavior for the vast majority of populations/modes. Figs. 5 and 6 depict the apparent activation energies calculated from this analysis that are associated with desorption and diffusion, respectively. In the sections below, the apparent activation energy trends and their mechanistic implications are discussed.

Apparent activation energy of desorption

Fig. 5 shows the calculated apparent activation energies of desorption for each population and protein-surface combination. It is important to recognize that the shortest-lived population, P1, represents the vast majority of all objects, and that virtually all monomeric protein objects fall within the P1 population. For all protein-surface combinations, the apparent activation energy associated with P1 was in the range of 2–4 kJ/mol, or $<2\ k_BT$. This is a major conclusion for this work; the energy barrier for removal of an isolated protein is extremely weak, regardless of the protein identity or surface hydrophobicity. In general, however, the apparent activation barriers associated with longer-lived populations P2, P3, and P4 (ranging from 2 to 12 kJ/mol) associated with protein oligomers increased systematically from that of P1. Intuitively, one would expect larger oligomers to occupy a greater surface area and therefore have stronger overall protein-surface interactions. This would facilitate more opportunities for favorable interactions (e.g., hydrogen bonding and van der Waals attractions) with a greater activation energy required for surface dissociation. These observations are consistent with the notion that monomers and dimers are typically very weakly bound, and that therefore surface fouling relies on the creation of larger oligomeric states.

The apparent activation energies for desorption from hydrophobic TMS were lower for BSA than for hydrophilic FS, and were similar for Fg on both surfaces. This would appear to be in contradiction to the literature observations that the net ensemble-averaged protein adsorption increases with increasing surface hydrophobicity, and that on average proteins tend to adhere more strongly to hydrophobic surfaces (3,4,36). A previously proposed rationale for this observation is that proteins unfold and spread more readily on hydrophobic surfaces (3,37). Wertz and Santore (10) observed that Fg relaxation to an irreversibly bound state on hydrophobic surfaces was extremely slow, with a characteristic spreading time of 1425 s. However, the residence times observed in this work were much shorter for all protein-surface combinations than that proposed spreading time, so there would appear to be insufficient time for isolated proteins (or small oligomers) to "spread" or unfold

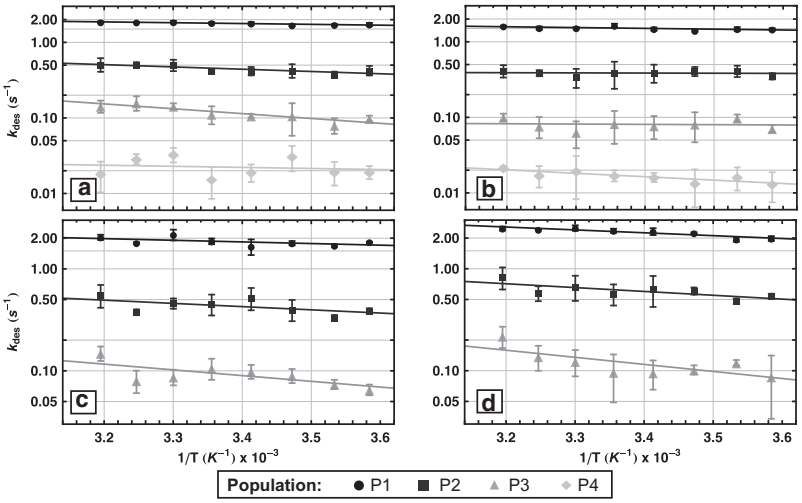

FIGURE 3 Arrhenius plots of desorption for the shortest lived population, P1; intermediate P2 and P3; and longest lived P4 as annotated. (*a*) BSA on FS, (*b*) BSA on TMS, (*c*) Fg on FS, and (*d*) Fg on TMS. Error bars correspond to the standard deviation of multiple measurements of $k_{des,i}$.

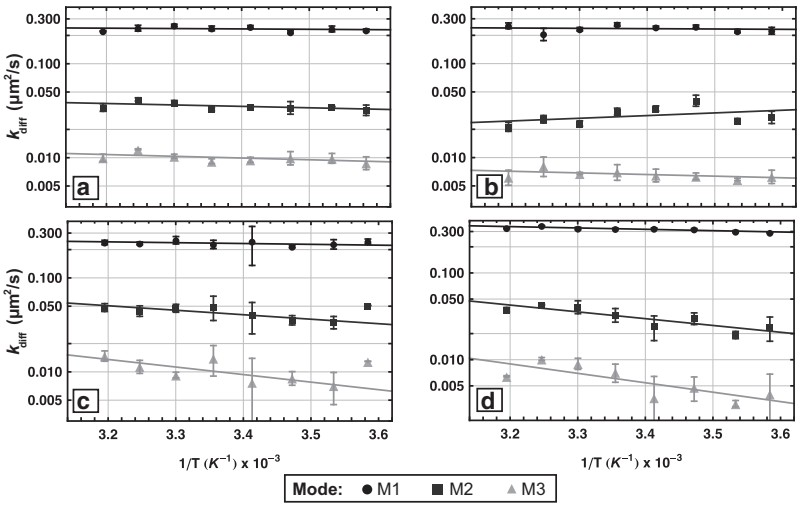

FIGURE 4 Arrhenius plots of diffusion for the fastest diffusion mode, M1, and successively slower M2, and M3 modes as annotated. (*a*) BSA on FS, (*b*) BSA on TMS, (*c*) Fg on FS, and (*d*) Fg on TMS. Error bars correspond to the standard deviation of multiple measurements of $k_{diff,j}$.

before desorption. Therefore, the small activation energies for desorption from TMS would appear to be consistent with the expected weak interactions between the hydrophobic surface and the native protein with predominantly hydrophilic exposure. This explanation also accounts for the observation that differences between BSA and Fg were fairly minimal on both hydrophilic and hydrophobic surfaces. Although BSA is a softer, globular protein that more readily undergoes conformational changes (4), the short surface residence times observed here suggest that unfolding does not occur extensively for short-lived species.

We suggest that the apparent inconsistency between previous bulk ensemble-averaged measurements (e.g., extremely slow relaxation and enhanced fouling of hydrophobic surfaces) and the data presented here provide valuable new insights into the mechanisms for protein layer formation. For example, our results show conclusively that, in the absence of protein-protein interactions, direct protein-surface interactions do not typically lead to irreversible adsorption and/or spreading or unfolding of monomers, dimers, etc. Instead, our results suggest that oligomers and aggregates are the long-lived species that ultimately lead to surface fouling. This is consistent with previous observations that protein surface behavior varies greatly with protein concentration (10,11).

It is therefore critical to focus on the ways in which surface chemistry may influence protein-protein interactions by promoting or inhibiting aggregation on the surface. For example, three different interactions are important in determining the mechanism and progression of layer formation: 1), direct protein-surface interactions in the absence of protein-protein interactions; 2), pairwise protein-protein interactions in the absence of protein-surface interactions; and 3), protein-surface interactions in the presence of protein-protein interactions (a three-body interaction). In this work we carefully studied the first type of interaction (isolated protein-surface interactions) and found that by itself, it is incapable of explaining layer formation phenomena, indicating that the second and third types of interactions must be important. In future work we will attempt to quantify these effects indirectly (by examining surface dynamics at higher bulk

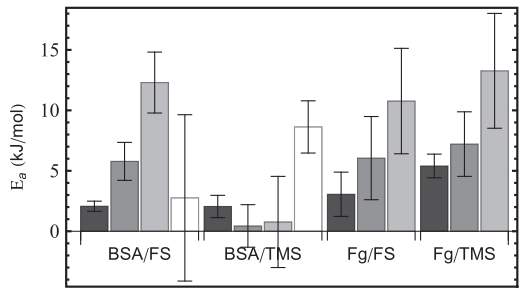

FIGURE 5 Apparent activation energies of desorption for P1 (*dark gray*), P2 (*gray*), P3 (*light gray*), and P4 (*white*) as annotated. Errors bars represent SEs associated with fitting Arrhenius temperature trends.

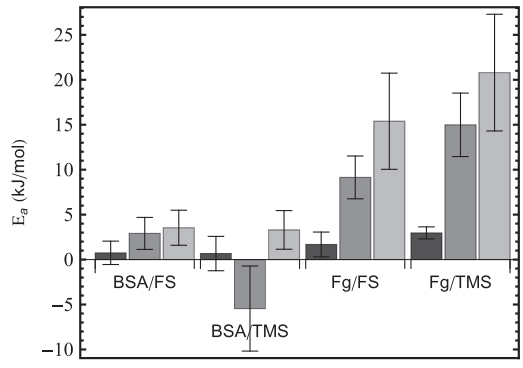

FIGURE 6 Apparent activation energies of diffusion for the fastest mode (M1, *dark gray*) and progressively slower modes (M2, *gray*; M3, *light gray*). Errors bars represent SEs associated with fitting Arrhenius temperature trends.

concentrations) and directly (by visualizing protein-protein collisions and associations).

Apparent activation energy of diffusion

Diffusive modes have been linked to multiple types of surface associations, molecular surface footprints, and the extent of molecule-surface associations (26,38). In the context of Fig. 1, these different types of associations lead hypothetically to different corrugations in the potential energy experienced by the adsorbate molecule as a function of position and orientation on the interfacial plane. For example, for ellipsoidal proteins (or protein oligomers), end-on and side-on associations have been proposed (8,10,26). Proteins can potentially switch between the two associations on a characteristic timescale, leading to motion characterized by multiple interspersed modes for a single object.

For small molecules, we previously found that mobile surface molecules exhibit two distinct mechanisms of diffusion: 1), a "sliding" or crawling mode in which a molecule stays in direct contact with the surface; or 2), a "flying" or partial-detachment mode in which a molecule briefly detaches from the surface during motion (24,28). These modes were characterized for fatty acid molecules on TMS, where a single hydrophobic tail-surface interaction and the associated surface-water interactions were believed to dictate the mode(s) of diffusion. With regard to large protein molecules, a larger number of surface contacts and more diverse variety of protein-surface interactions presumably lead to the more-complex behavior observed here. We therefore hypothesize that the heterogeneity associated with protein surface diffusion results from multiple surface association configurations and mechanisms.

Fig. 6 shows the measured apparent activation energies for diffusion. As with the activation energies associated with desorption of monomers (P1 in Fig. 5), the activation energies for the diffusion of the fastest mode M1 (often associated with protein monomers and presumably weaker interactions) were again very small in magnitude, typically in the range of 0–2 k_BT. Thus our data consistently show that regardless of the protein identity or the surface chemistry, the energy barriers associated with the removal and/or mobility of weakly bound protein monomers or oligomers were extremely small.

The activation energies for the slower modes (M2 and M3), however, exhibited different trends for each surface-protein combination. For Fg on FS, the activation energies associated with diffusion and desorption were similar in magnitude. One might expect populations/modes with similar activation energies to correspond to similar protein-surface interactions. However, as discussed above, a given desorption activation energy is not necessarily correlated to a particular diffusion activation in these data. The fact that these energy barriers did correspond (for Fg on FS) suggests that partial desorption represents the more likely type of diffusion on FS for Fg. Due to the potential for hydrogen bonding with hydrophilic surfaces, stronger surface-solution interactions on hydrophilic surfaces would make displacement of surface-bound water molecules less favorable for hypothetical sliding/crawling modes. Thus, partial-desorption diffusive modes may be more energetically favorable compared with sliding/crawling modes on hydrogen-bonding surfaces.

The large discrepancy between BSA and Fg diffusion energies on TMS suggests that diffusion on hydrophobic surfaces is highly protein-dependent. For BSA, the diffusive modes for nearly all modes were activationless (within experimental error), whereas the diffusive modes for Fg exhibited relatively large activation barriers. This difference suggests that different diffusive modes can result from qualitatively different mechanisms, and that the relative favorability of these diffusion mechanisms is protein-dependent. For example, we propose that BSA primarily diffuses on TMS via a sliding mode, whereas Fg motion is dominated by the flying mode. This hypothesis is supported not only by the trends in the activation energies but also by the proportion of steps associated with the various modes. In particular, BSA motion on TMS is strongly dominated by the slowest mode (M3). Fg motion was more balanced between modes, but the fastest mode (M1) was the most populated. Sliding modes would appear to be favored on homogeneous hydrophobic surfaces because of the absence of specific short-range interactions (e.g., hydrogen bonding), and this should lead to very small corrugations in the surface energy. This might explain the low apparent activation energies of BSA on TMS and the prevalence of fast-moving Fg on TMS.

Activation barriers are small in absolute terms

The measured activation energies over the 6–40°C temperature range were found to be relatively small for all protein-surface combinations and types of dynamics. Previous work in our laboratory measured activation energies of 5–20 kJ/mol associated with the dynamics of small fatty acid probe molecules (i.e., for adsorption on FS and diffusion on TMS) (24,25). Multiple protein-surface interactions and surface-solvent interactions are expected to contribute to the energy required to move or desorb a protein from the interface. Nevertheless, virtually all of the apparent activation barriers for BSA and Fg were similar or smaller than the barriers for a single fatty acid molecule, or even that of a single hydrogen bond (~15–20 kJ/mol) (39,40).

This finding is puzzling yet not unprecedented. In previous studies, investigators quantified protein-surface interaction free energies using solution depletion (12,14,29,30,41), molecular dynamics simulations (5), and other methods (12,42). Many of these studies indicated small free energies associated with protein adsorption, on the order of 10–18 kJ/mol. For example, the free energy of adsorption of lysozyme and Fg was theoretically and

experimentally calculated to be smaller or equal to that of a single hydrogen bond for the entire protein at low surface coverage (42,43). Similarly, in other studies, several types of proteins (ranging from 10 to 100 kDa) were found to have a low apparent free energy of adsorption on hydrophobic surfaces, on the order of 10–15 kJ/mol (14,30). This reinforces the idea that isolated protein-surface interactions are relatively weak and that therefore protein-protein interactions must be important in explaining protein-resistant surface mechanisms. Other work in our laboratory incorporating higher concentrations of unlabeled protein provided insight into the role of protein-protein interactions on the layer formation of BSA at the oil-water interface (44). In these experiments, the distribution of diffusion coefficients was observed to broaden, and the spatial distribution of adsorption rates became more heterogeneous with time, indicating aggregation at the interface (44). It is possible that these phenomena may also be relevant for other proteins and at other interfaces.

CONCLUSIONS

The ability to observe single-molecule protein-surface interactions over a wide temperature range demonstrates the power of single-molecule tracking to isolate complicated protein-surface behaviors into elementary component mechanisms, as well as to determine the effective energies associated with protein interfacial dynamics. The omnipresent proof of heterogeneity in every aspect of these experiments highlights the need for more sophisticated analysis of protein-surface interactions, and calls into question many mechanistic interpretations that have been made on the basis of ensemble-averaged methods.

Regardless of the protein identity or surface chemistry, the vast majority of individual protein objects exhibited short residence times (<1 s), relatively fast motion, and weak surface binding at low protein concentrations where protein-protein interactions are insignificant. Although this is consistent with a growing literature on protein-surface interactions, it stands in strong contrast to previous interpretations that often regarded adsorbed proteins as irreversibly bound and immobilized. In contrast, our observations directly show that isolated protein molecules quickly desorb from the surface in the absence of protein-protein interactions, and that the formation of larger oligomers/clusters is necessary to achieve the longer residence times that ultimately lead to surface fouling. This suggests that although isolated native protein-surface interactions play some role in protein adsorption at the interface, they are not the dominant drivers for surface protein fouling. Thus, it is critically important to consider the effects associated with populations of preformed oligomers in solution as well as the dynamic formation of oligomers on the surface, especially when considering the higher protein solution concentrations that are necessary for protein fouling. In particular, interactions between proteins within the surface layer may be strongly influenced by the physicochemical properties of the surface, representing a complex "three-body" problem.

Although surface residence times were relatively insensitive to the details of the protein-surface interaction, the mechanisms of surface mobility exhibited a complex dependence on these interactions. We speculate that these details of surface mobility may play a critical role in defining the process of protein aggregation on the surface. For example, proteins that engage primarily in sliding/crawling diffusion (and surfaces that encourage this mode of diffusion) are more likely to lead to protein-protein collisions that can lead to the formation of surface aggregates. Nevertheless, we suggest that the effects of surface chemistry on protein surface mobility, and more generally on protein-protein clustering, may be a critical determinant of protein layer formation and surface fouling.

SUPPORTING MATERIAL

Supplementary Materials and Methods, Data Analysis, Data Fitting, Results and Discussion, two tables, two figures, and references are available at http://www.biophysj.org/biophysj/supplemental/S0006-3495(12)00501-2.

This work was supported by the National Science Foundation (CHE-0841116), the National Science Foundation Industry/University Cooperative Research Center for Membrane Science, Engineering and Technology (IIP1034720), the U.S. Department of Energy (DE- SC0001854), and the National Institute of General Medical Sciences (1F32GM091777-02).

REFERENCES

1. Wisniewski, N., and M. Reichert. 2000. Methods for reducing biosensor membrane biofouling. *Colloids Surf. B Biointerfaces.* 18:197–219.
2. Roach, P., D. Farrar, and C. C. Perry. 2005. Interpretation of protein adsorption: surface-induced conformational changes. *J. Am. Chem. Soc.* 127:8168–8173.
3. Rabe, M., D. Verdes, and S. Seeger. 2011. Understanding protein adsorption phenomena at solid surfaces. *Adv. Colloid Interface Sci.* 162:87–106.
4. Nakanishi, K., T. Sakiyama, and K. Imamura. 2001. On the adsorption of proteins on solid surfaces, a common but very complicated phenomenon. *J. Biosci. Bioeng.* 91:233–244.
5. Jamadagni, S. N., R. Godawat, and S. Garde. 2011. Hydrophobicity of proteins and interfaces: insights from density fluctuations. *Annu. Rev. Chem. Biomol. Eng.* 2:147–171.
6. Ostuni, E., B. A. Grzybowski, …, G. M. Whitesides. 2003. Adsorption of proteins to hydrophobic sites on mixed self-assembled monolayers. *Langmuir.* 19:1861–1872.
7. Gray, J. J. 2004. The interaction of proteins with solid surfaces. *Curr. Opin. Struct. Biol.* 14:110–115.
8. Daly, S. M., T. M. Przybycien, and R. D. Tilton. 2003. Coverage-dependent orientation of lysozyme adsorbed on silica. *Langmuir.* 19:3848–3857.
9. Wertz, C. F., and M. M. Santore. 1999. Adsorption and relaxation kinetics of albumin and fibrinogen on hydrophobic surfaces: single-species and competitive behavior. *Langmuir.* 15:8884–8894.

10. Wertz, C. F., and M. M. Santore. 2002. Fibrinogen adsorption on hydrophilic and hydrophobic surfaces: Geometrical and energetic aspects of interfacial relaxations. *Langmuir.* 18:706–715.

11. Siegel, R. R., P. Harder, …, G. M. Whitesides. 1997. On-line detection of nonspecific protein adsorption at artificial surfaces. *Anal. Chem.* 69:3321–3328.

12. Fainerman, V. B., R. Miller, …, M. Michel. 2006. Reversibility and irreversibility of adsorption of surfactants and proteins at liquid interfaces. *Adv. Colloid Interface Sci.* 123-126:163–171.

13. Vieira, E. P., S. Rocha, …, M. A. Coelho. 2009. Adsorption and diffusion of plasma proteins on hydrophilic and hydrophobic surfaces: effect of trifluoroethanol on protein structure. *Langmuir.* 25:9879–9886.

14. Noh, H., S. T. Yohe, and E. A. Vogler. 2008. Volumetric interpretation of protein adsorption: ion-exchange adsorbent capacity, protein pI, and interaction energetics. *Biomaterials.* 29:2033–2048.

15. Ostuni, E., R. G. Chapman, …, G. M. Whitesides. 2001. A survey of structure-property relationships of surfaces that resist the adsorption of protein. *Langmuir.* 17:5605–5620.

16. Sigal, G. B., M. Mrksich, and G. M. Whitesides. 1998. Effect of surface wettability on the adsorption of proteins and detergents. *J. Am. Chem. Soc.* 120:3464–3473.

17. Prime, K. L., and G. M. Whitesides. 1991. Self-assembled organic monolayers: model systems for studying adsorption of proteins at surfaces. *Science.* 252:1164–1167.

18. Jackler, G., R. Steitz, and C. Czeslik. 2002. Effect of temperature on the adsorption of lysozyme at the silica/water interface studied by optical and neutron reflectometry. *Langmuir.* 18:6565–6570.

19. Vogler, E. A. 2012. Protein adsorption in three dimensions. *Biomaterials.* 33:1201–1237.

20. Honciuc, A., D. J. Baptiste, …, D. K. Schwartz. 2009. Solvent dependence of the activation energy of attachment determined by single molecule observations of surfactant adsorption. *Langmuir.* 25:7389–7392.

21. Kwok, K. C., K. M. Yeung, and N. H. Cheung. 2007. Adsorption kinetics of bovine serum albumin on fused silica: population heterogeneities revealed by single-molecule fluorescence microscopy. *Langmuir.* 23:1948–1952.

22. Yeung, K. M., Z. J. Lu, and N. H. Cheung. 2009. Adsorption of bovine serum albumin on fused silica: Elucidation of protein-protein interactions by single-molecule fluorescence microscopy. *Colloids Surf. B Biointerfaces.* 69:246–250.

23. Honciuc, A., A. W. Harant, and D. K. Schwartz. 2008. Single-molecule observations of surfactant diffusion at the solution-solid interface. *Langmuir.* 24:6562–6566.

24. Honciuc, A., and D. K. Schwartz. 2009. Probing hydrophobic interactions using trajectories of amphiphilic molecules at a hydrophobic/water interface. *J. Am. Chem. Soc.* 131:5973–5979.

25. Honciuc, A., A. L. Howard, and D. K. Schwartz. 2009. Single molecule observations of fatty acid adsorption at the silica/water interface: activation energy of attachment. *J. Phys. Chem. C.* 113:2078–2081.

26. Walder, R., and D. K. Schwartz. 2010. Single molecule observations of multiple protein populations at the oil-water interface. *Langmuir.* 26:13364–13367.

27. Kastantin, M., B. B. Langdon, …, D. K. Schwartz. 2011. Single-molecule resolution of interfacial fibrinogen behavior: effects of oligomer populations and surface chemistry. *J. Am. Chem. Soc.* 133:4975–4983.

28. Walder, R., N. Nelson, and D. K. Schwartz. 2011. Single molecule observations of desorption-mediated diffusion at the solid-liquid interface. *Phys. Rev. Lett.* 107:156102.

29. Sarkar, D., and D. K. Chattoraj. 1996. Kinetics of desorption of proteins from the surface of protein-coated alumina by various desorbing reagents. *J. Colloid Interface Sci.* 178:606–613.

30. Noh, H., and E. A. Vogler. 2006. Volumetric interpretation of protein adsorption: mass and energy balance for albumin adsorption to particulate adsorbents with incrementally increasing hydrophilicity. *Biomaterials.* 27:5801–5812.

31. Steinbach, P. J., R. Ionescu, and C. R. Matthews. 2002. Analysis of kinetics using a hybrid maximum-entropy/nonlinear-least-squares method: application to protein folding. *Biophys. J.* 82:2244–2255.

32. Kastantin, M., and D. K. Schwartz. 2012. Distinguishing positional uncertainty from true mobility in single-molecule trajectories that exhibit multiple diffusive modes. *Microsc. Microanal.* In press.

33. Tilton, R. D., A. P. Gast, and C. R. Robertson. 1990. Surface diffusion of interacting proteins. Effect of concentration on the lateral mobility of adsorbed bovine serum albumin. *Biophys. J.* 58:1321–1326.

34. Tilton, R. D., C. R. Robertson, and A. P. Gast. 1990. Lateral diffusion of bovine serum albumin adsorbed at the solid-liquid interface. *J. Colloid Interface Sci.* 137:192–203.

35. Nygren, H., S. Alaeddin, …, K. E. Magnusson. 1994. Effect of surface wettability on protein adsorption and lateral diffusion. Analysis of data and a statistical model. *Biophys. Chem.* 49:263–272.

36. Ostuni, E., L. Yan, and G. M. Whitesides. 1999. The interaction of proteins and cells with self-assembled monolayers of alkanethiolates on gold and silver. *Colloids Surf. B Biointerfaces.* 15:3–30.

37. Wertz, C. F., and M. M. Santore. 2001. Effect of surface hydrophobicity on adsorption and relaxation kinetics of albumin and fibrinogen: single-species and competitive behavior. *Langmuir.* 17:3006–3016.

38. Jamadagni, S. N., R. Godawat, and S. Garde. 2009. How surface wettability affects the binding, folding, and dynamics of hydrophobic polymers at interfaces. *Langmuir.* 25:13092–13099.

39. Curtiss, L. A., D. J. Frurip, and M. Blander. 1979. Studies of molecular association in H2O and D2O vapors by measurement of thermal-conductivity. *J. Chem. Phys.* 71:2703–2711.

40. Feyereisen, M. W., D. Feller, and D. A. Dixon. 1996. Hydrogen bond energy of the water dimer. *J. Phys. Chem.* 100:2993–2997.

41. Noh, H., and E. A. Vogler. 2006. Volumetric interpretation of protein adsorption: partition coefficients, interphase volumes, and free energies of adsorption to hydrophobic surfaces. *Biomaterials.* 27:5780–5793.

42. Wei, Y., and R. A. Latour. 2010. Correlation between desorption force measured by atomic force microscopy and adsorption free energy measured by surface plasmon resonance spectroscopy for peptide-surface interactions. *Langmuir.* 26:18852–18861.

43. Latour, R. A. 2006. Thermodynamic perspectives on the molecular mechanisms providing protein adsorption resistance that include protein-surface interactions. *J. Biomed. Mater. Res. A.* 78:843–854.

44. Walder, R., and D. K. Schwartz. 2011. Dynamics of protein aggregation at the oil-water interface characterized by single molecule TIRF microscopy. *Soft Matter.* 7:7616–7622.